

## **[Supplementary Material]**

### **What lies beneath ... Late Glacial human occupation of the submerged North Sea landscape**

Luc Amkreutz<sup>1</sup>, Alexander Verpoorte<sup>2,\*</sup>, Andrea Waters-Rist<sup>2</sup>, Marcel Niekus<sup>3</sup>, Vivian van Heekeren<sup>2</sup>, Alie van der Merwe<sup>4</sup>, Hans van der Plicht<sup>2,5</sup>, Jan Glimmerveen<sup>2</sup>, Dick Stapert<sup>6</sup> & Lykke Johansen<sup>6</sup>

<sup>1</sup> *National Museum of Antiquities, Rapenburg 28, 2311 EW Leiden, The Netherlands*

<sup>2</sup> *Faculty of Archaeology, Leiden University, Einsteinweg 2, 2333 CC Leiden, The Netherlands*

<sup>3</sup> *Stichting STONE/Foundation for Stone Age research in the Netherlands, c/o Lopendediep 28, 9712 NW Groningen, The Netherlands*

<sup>4</sup> *Department of Anatomy, Embryology and Physiology, Academic Medical Center, Meibergdreef 9, 1105 AZ Amsterdam, The Netherlands*

<sup>5</sup> *Centre for Isotope Research, Groningen University, Nijenborgh 4, 9747 AG Groningen, The Netherlands*

<sup>6</sup> *Ossewei 6, 9751 SC Haren, The Netherlands*

*\* Author for correspondence (Email: a.verpoorte@arch.leidenuniv.nl)*

## **S1. The Human Parietal Bone**

### **Introduction**

The bone was retrieved during fishing activities of the “Scheveningen 18” vessel, on June 6, 2013. The find location is 52.01 degrees North and 03.51 degrees East, just south of the Eurogeul, the main approach to Rotterdam Harbor; north of the aggregates extraction area for the Second Maasvlakte, the latest extension of the Rotterdam Harbour. It was donated to the Museum of Antiquities, Leiden, The Netherlands, where it was sampled for radiocarbon dating and stable isotope analysis by Prof. Dr. H. van der Plicht (CIO, Groningen) on September 27, 2013. Afterwards the bone was preserved and stored under inventory number U 2013/6.1.

### **Local geology**

The find location is part of the Southern Bight of the North Sea. The area is situated on the shoulder between the depocenter of the Southern North Sea Basin and the erosional zones to

the south. The base of the Quaternary sequence is formed by Early Pleistocene fine sands. Deeply incised features in the Early Pleistocene deposits contain sands with gravels of the Urk Formation and are overlain by gravelly sands deposited during the Saalian deglaciation. These sediments are covered by Weichselian-age fluvial sands. The upper units are gravelly sands deposited by the Rhine-Meuse-system, dated onshore to an absolute age range of 24,000 to 9,000 BP (Hijma *et al.* 2012). Occasionally, pumice of the Laachersee eruption dated to around 12,900 BP is found (Bronk Ramsey *et al.* 2015). Wind-blown deposits, comprising isolated dune complexes and coversands, have been documented locally. The Late Glacial sedimentary units are overlain by Holocene marine deposits with a coarse lag deposit at the base and the Basal Peat Bed (Hijma *et al.* 2012). The human parietal bone was probably eroded from local Late Glacial sediments or from the Holocene lag deposit that contains reworked glacial sediments.

## **Methods**

The sample for radiocarbon and stable isotope analyses was taken before preservation and description of the bone. The bone sample measured approximately 4.3 by 2.5mm and ran from the coronal border to the sphenoidal angle. It contained sufficient material for radiocarbon dating and stable isotope analysis.

The bone was investigated macroscopically at the National Museum of Antiquities, Leiden, The Netherlands. Length and width measurements were taken with a digital caliper (to 0.1mm). Measurements of thickness (outer plate, diploë, inner plate) were derived from a CT scan of the element conducted at the Academic Medical Centre (AMC), Amsterdam. Measurements are provided in table 1 and 2. The scan was performed on a Philips Brilliance 64 CT scanner (Philips Medical Systems Best) set at 199 mAs and 120 kV with a slice thickness of 1mm. A virtual 3D reconstruction of the element was created according to de Boer (2011) by using AMIRA version 5.5. Finally, a dino-lite AM7013MT was used to better visualise and photograph the area of bryozoan occupation and slight porosity on the ectocranial surface (described below) using low magnification (15 to 65×).

## **Description and Preservation of the Bone**

The bone is an approximately 70% complete human left parietal. It is missing several centimeters of its anterior edge, including the frontal angle (and thus the landmark bregma), coronal suture, and the sphenoidal angle (and thus the landmark pterion). The edges of the mastoid angle portion of the bone are slightly weathered but intact. The lambdoidal suture is

completely intact and the sagittal suture is approximately 75% intact. Both these sutures are heavily inter-digitated with small pieces of adjacent bones (i.e. the occipital bone in the lambdoidal suture and right temporal bone in the sagittal suture) interlocked in several locations. The squamosal suture is approximately 65% intact. A parietal foramen is present towards the posterior end of the sagittal suture. This is a normal anatomical variant, reported as present in 20% (Boyd 1930) to 60% (Reinhard & Rösing 1985) of individuals. On the endocranial surface three granular foveolae are present in the sagittal groove, one of which is moderately large (5.6 by 2.6mm). These foveolae are for arachnoid granulations that function to circulate cerebrospinal fluid (Scheuer & Black 2000).

The ectocranial surface of the parietal bone has an overall smooth surface. There are several small postmortem micro-cracks on the endocranial surface around the parietal eminence. There is a large postmortem crack, 64mm long, running from the anterior side (43mm superior to the squamosal suture) to around the middle of the bone, visible on the ecto- and endocranial surfaces. This crack, as well as some of the smaller ones, probably occurred when the bone dried after having been removed from seawater. The ectocranial surface generally has a brown colour with some grey-brown and white spots. The grey brown spots are probably caused by postmortem flaking, which has subsequently been smoothed by the museum preservative. The white spots are the remains of colonies of bryozoans, indicating that the bone has been in the seawater (Faasse, pers. comm. 2015: the colonies could have grown within a month of deposition). These bryozoans are also present on the endocranial surface of the bone. In addition, there is slight postmortem flaking present on the endocranial surface.

The endocranial surface of the parietal bone has a bumpier surface. The bone's thickness at different locations ranges from ~1.0 to ~8.0mm and this variable thickness is manifest on the inner surface. The cortical bone overlaying the bumpy endocranial surface is smooth and has a yellow-brown to dark-brown colour. Two complete branches of meningeal grooves are present, of which the posterior branch is most distinct. A third branch of meningeal grooves is partially evident along the broken anterior border. Some small post-mortem cracks appear in the meningeal grooves, especially where the bone is thinnest.

Overall, the bone closest belongs to weathering stage '2', meaning that cracking and flaking are visible (Buikstra & Ubelaker 1994). However, the flaking on this bone is slight and does affect an extensive amount of the surface, so most of the bone displays a category '1' designation, wherein only cracking is present.

### **Age-at-Death Estimation**

The overall size of the bone is not particularly useful in determining if it derives from a subadult (<18 years) or adult (18+ years), because the size of the bone is largely set by four years of age (Young 1957). The thickness of the bone, however, suggests it is from an adult, with many studies examining the effects of growth, age, sex, and ethnicity on cranial thickness (e.g. Todd 1924; Twiesselmann 1941; Getz 1960; Angel 1971; Adeloje *et al.* 1975; Ross *et al.* 1998; Jung *et al.* 2003; Li *et al.* 2007). The thickness of the mid-sagittal area of this parietal is 6.1mm (Table 2), which is equal to the mean median sagittal arc thickness (6.1±0.7mm) of modern adult Europeans (Young 1957). It is unfortunate that the landmark bregma is absent, as several studies have determined its mean thickness in both males and females of various age groups. In this specimen, the closest point to bregma along the sagittal suture has a thickness of 5.2mm. In Holocene-period adults of European origin or descent, bregma thickness has been determined for adults from the French Neolithic (6.8mm; n=15), and the French (5.4mm; n=200), Belgian (5.3mm; n=200) and American post-industrial period (5.9 mm; n=445 post-industrial period (Twiesselmann 1941; Roche 1953). In early modern human fossils from Europe, 17 bregma yielded thickness data (Lieberman 1996), which range from 12.0mm (La Cotte de St. Brelade) to 3.5mm (Mladec 1), with an average thickness of 7.4 ±2.0mm.

Fortunately, many studies have also determined the mean thickness of the parietal eminence, which is intact in this specimen and measures 6.2mm (Table 2). In Holocene-period adults of European origin or descent, parietal eminence thickness has been determined for populations from the French Neolithic (6.7mm; n=15) and French (5.7mm; n=200), Belgian (5.7mm; n=200) (Twiesselmann 1941), and American post-industrial period (3.6mm; n=445; Roche 1953 and 2.9mm; n=32; Todd 1924). In early modern human fossils from Europe, 28 samples have yielded parietal eminence thickness data (Lieberman 1996), which range from 14.0mm (Boskop) to 3.5mm (Mladec 1), with an average thickness of 7.4±2.5mm. Based on these data, Lieberman (1996) found that Pleistocene modern humans have significantly thicker parietal eminences than Holocene modern humans (see Kennedy *et al.* 1991 for a compilation of parietal thickness data from Pliocene and Pleistocene bipedal hominins). The thickness of the parietal eminence of this specimen fits well within the range of adult parietal eminence thicknesses of fossils of similar age, and suggests that the individual was an adult. While it is not possible to provide a narrower estimate on the basis of temporal bone thickness, cranial suture closure may refine the age-at-death estimate.

The individual was likely a young or middle aged-adult (18-49 years). This broad estimate is based upon the fact that cranial sutures fuse and become obliterated with increasing age. Both endocranial and ectocranial suture fusion was minimally evident in this bone. Four specific suture locations could be examined for state of closure – the mid-lambdoidal, lambda, obelion, and anterior sagittal - using a four-stage scale (0=open; 1=minimal closure; 2=significant closure; 3=complete obliteration) (Meindl and Lovejoy 1985). Only the mid-lambdoidal suture showed any closure (stage 10), with all other suture points being completely open. The fifth suture site at the bregma is required for the method of Meindl and Lovejoy (1985) to be applied to estimate a specific age range. This site is unfortunately absent. If we set bregma at the maximum value of three, however, we can derive the theoretically maximum score. The specimen could not have been older than this estimate. Given a composite vault score of four (1 from mid-lambdoidal and 3 from bregma), an age range of 22 to 45 years is suggested (Meindl & Lovejoy 1985). Finally, Barber *et al.* (1995) found that the number of granular foveolae in the parietal increases with age in European and African American samples. This finding, as well as an increase in the depth of the foveolae with age, was also noted by Basmajian (1952). Unfortunately, the overlap in ranges of different age groups was substantial, and the method needs further testing and substantiation using larger samples of known age, sex and ethnicity before it is applicable to estimate age in single specimens of unknown sex and ethnicity.

### **Sex Estimation**

It is very difficult to estimate sex from a single parietal bone because it possesses few sexually dimorphic traits, and even those that are present are not very diagnostic. Females are more likely to have parietal (and frontal) bossing (Wilkinson 2004). As such, parietal bossing has been viewed as trait indicating female sex (i.e. Loth & İşcan 2000), although given the regularity with which it is observed on male crania, some authors state that it should not be used in sex estimation (i.e. Dolinak *et al.* 2005). An additional problem with using parietal bossing in sex estimation is its very high intra-observer error, with a reliability gamma score of only 0.21 (perfect is 1.00) (Walrath *et al.* 2004). In this specimen, slight parietal bossing is present, but it is not pronounced, warranting an indeterminate score in regards to sex. Males often have larger crania than females, with more pronounced muscle markings. The parietal itself, however, has been found to be either not significantly different in length or breadth between males and females, or minimally different in size to a degree that is not useful for the estimation of sex (Keen 1950). Furthermore, the parietal does not possess areas

which respond markedly to overlying muscularity. There are the superior and inferior temporal lines, which demarcate the borders of the temporalis muscle used in mastication (the former giving attachment to the temporal fascia, and the latter indicating the upper limit of the temporalis muscle) (Washburn 1947). These features are, however, usually slight and not particularly useful in the estimation of sex. Although the superior and inferior temporal lines are not visible in this specimen (which is more consistent with a female morphology), this is not sufficiently diagnostic to base a sex estimate.

The thickness of the parietal bone, or thickness of its diploë, has been examined in studies looking for sex differences, among others (i.e. Pensler & McCarthy 1985; Li *et al.* 2007; Hatipoglu *et al.* 2008). Based on CT scans of 3000 individuals Li. *et al.* (2007) found that overall parietal thickness was 5.37mm for females and 5.58cm for males - a difference, that while statistically significant, is too slight upon which to base a sex estimation. Hatipoglu *et al.* (2008) concluded that there was not a significant relationship between sex and parietal diploë thickness (although did support the earlier mentioned finding of increased diploë thickness with age), with the increased thickness occurring at different rates in males and females. Pensler and McCarthy (1985) concluded that weight, ethnicity, age, and sex all affect cranial thickness significantly, but are difficult to disentangle. Given that the age or weight of the individual are unknown, and that we cannot be sure about their ancestry (although European is supposed based upon the populations known to present in this temporal-geographic period), it is not possible to use cranial thickness to estimate sex. Moreover, the skulls of Pleistocene humans were more robust than those of modern-day *Homo sapiens* (Kennedy 1991; Gauld 1996; Lahr & Wright 1996; Lieberman 1996; also see Verhaegena and Munro 2011); even if a sexually dimorphic marker was present in the parietal bone of modern populations, the data could not be straightforwardly applied to estimate sex from this parietal bone.

### **Morphological Abnormality and Pathology**

The bone does not display any osseous anatomical anomalies (i.e. parietal notch remnant, parietal fontanelle, enlarged parietal foramina) or major pathological lesions (i.e. osteodystrophy). On the ectocranial surface there are, however, very fine ‘pin-head’ shallow pits in a diffuse band running along the sagittal suture. The pitted band begins approximately two centimeters from the lambdoidal suture and extends to the bone’s termination at the postmortem coronal edge break. The pitting is most prominent and concentrated in the area lateral to the parietal foramen (approximately four centimeters from the coronal edge), and in

an area approximately one and a half centimeters from the coronal edge. The CT scan reveals no marked expansion of the diploic space, or change in the organisation of the trabeculae in the area with pitting. The ratio of diploic to cortical plate space in this area is 208% (mid-sagittal, posterior mid-sagittal, and lambda combined). The outer table is not significantly thinner than the surrounding areas and the inner table is similarly unaffected.

Such pitting can be associated with a condition commonly encountered in paleopathology known as porotic hyperostosis. Pronounced cases of porotic hyperostosis have been found in several hominin fossils (i.e. Bräuer *et al.* 2003; Vercellotti *et al.* 2010; also see Spoor *et al.* 1998 and Curnoe & Brink 2010 for possible cases) with the oldest example from an approximately two-year-old child from the 1.5-million-year-old Sam Howard Korongo site, in Olduvai Gorge, Tanzania (Dominguez-Rodrigo *et al.* 2012). Porotic hyperostosis, seen mostly in subadults, has many different causes. It can be caused by the body's response to inadequate iron because of insufficient iron intake or absorption, and/or insufficient, malformed or damaged red blood cells. This causes the erythropoietic potential of the vault diploë to be put into action to create more red blood cells, causing expansion and dis- or reorganisation of the diploë, and pitting and porosity of the external cortex (Ortner 2003). Anaemic diseases that can cause porotic hyperostosis include those that are genetic (e.g. thalassaemia, sickle-cell anaemia, some megaloblastic forms) and those that are acquired via a dietary deficiency (i.e. dietary iron deficiency), absorptive deficiency (e.g. due to parasitic infection or chronic blood loss), the abnormal haemolytic breakdown of red blood cells (e.g. due to malaria), or the production of immature, dysfunctional red blood cells in megaloblastic anaemia related to folate and vitamin B12 deficiencies (Stuart-Macadam 1992; Walker *et al.* 2009). The hallmark features of porotic hyperostosis are resorptive thinning of the outer plate, widening of the diploic space, diploic disorganization or reorganisation - especially taking on a 'hair-on-end' appearance - and a granular (porotic) appearance to the vault on radiographic images (Stuart-Macadam 1987; Ortner 2003). The ratio of diploë thickness to cortical thickness (inner plus outer plate) has been suggested as an indicator of porotic hyperostosis, with an index value about 230% indicating pathological expansion of the diploic space (Stuart-Macadam 1987). Given that this specimen only possesses slight pitting, and none of these other features, and that it has a non-pathological diploë to cortical thickness ratio, it is not appropriate to state that this bone has evidence of active porotic hyperostosis. The pitting could be indicative of a largely healed porotic hyperostotic episode, but other conditions that could account for the pitting cannot be ruled out. For example, the pitting may be the healed remnants of scalp inflammation (caused by trauma - for which there is no bony evidence in this specimen - or

infection) (Schultz *et al.* 2001). Vitamin C deficiency (scurvy) and vitamin D deficiency (rickets/osteomalacia) have also been associated with porosity of the cranial vault, without changes to the underlying diploë, although other osseous changes can occur which are not present on this bone (e.g. bony evidence of subdural haematomas in scurvy and poorly mineralised trabeculae in rickets) (Ortner 2003; McIlvaine 2013). In summary, the etiology of these pits is unknown, but they could have formed from conditions that cause anaemia (e.g. dietary or gastrointestinal induced anaemia, genetic anaemia, malaria), as well as, scurvy, rickets, or scalp inflammation as a result of trauma or infection. The individual survived the pathological insult such that the lesion is quite well-healed.

## References

- ADELOYE, A, KATTAN, K.R. & F.N. SILVERMAN. 1975. Thickness of the normal skull in the American Blacks and Whites. *American Journal of Physical Anthropology* 43(1): 23-30.
- ANGEL, L. 1971. Skull vault thickness variation. *American Journal of Physical Anthropology* 35: 272.
- BARBER, G., L. SHEPSTONE & J. ROGERS. 1995. A methodology for estimating age at death using arachnoid granulation counts. *American Journal of Physical Anthropology Supplement* 20: 61.
- BASMAJIAN, J.V. 1952. The Depressions for the Arachnoid Granulations as a Criterion of Age. *The Anatomical Record* 112: 843-847.
- DE BOER, B.A., A.T. SOUFAN, J. HAGOORT, T.J. MOHUN, M.J. VAN DEN HOFF, A. HASMAN, F.P. VOORBRAAK, A.F. MOORMAN & J.M. RUIJTER. 2011. The interactive presentation of 3D information obtained from reconstructed datasets and 3D placement of single histological sections with the 3D portable document format. *Development* 138(1): 159-67.
- BOYD, G.I. 1930. The emissary foramina in the crania of man and anthropoids. *Journal of Anatomy* 65: 108-121.
- BRAÜER, G., C. GRODEN, G. DELLING, K. KUPCZIK, E. MBUA & M. SCHULTZ. 2003. Pathological alterations in the archaic *Homo sapiens* cranium from Eliye Springs, Kenya. *American Journal of Physical Anthropology* 120(2): 200-204.
- BRONK RAMSEY, C., P.G. ALBERT, S.P.E. BLOCKLEY, M. HARDIMAN, R.A. HOUSLEY, C.S. LANE, S. LEE, I.P. MATTHEWS, V.C. SMITH & J. LOWE. 2015. Improved age estimates for key Late Quaternary European tephra horizons in the RESET lattice. *Quaternary Science Reviews* 118: 18-32.

- BUIKSTRA, J.E. & D.H. UBELAKER (eds). 1994. *Standards for data collection from human skeletal remains: seminar at the Field Museum of Natural History*. Fayetteville, AR: Arkansas Archaeological Survey.
- CURNOE, D. & J. BRINK. 2010. Evidence of Pathological Conditions in the Florisbad Cranium. *Journal of Human Evolution* 59: 504-513.
- DOMÍNGUEZ-RODRIGO, M., T.R. PICKERING, F. DIEZ-MARTÍN, A. MABULLA, C. MUSIBA, G. TRANCHO, E. BAQUEDANO, H.T. BUNN, D. BARBONI, M. SANTONJA, D. URIBELARREA, G.M. ASHLEY, M. DEL SOL MARTINEZ-AVILA, R. BARBA, A. GIDNA, J. YRAVEDRA & C. ARRIAZA. 2012. Earliest Porotic Hyperostosis on a 1.5-Million-Year-Old Hominin, Olduvai Gorge, Tanzania. *PLoS ONE* 7(10): e46414. doi:10.1371/journal.pone.0046414.
- DOLINAK, D., E. MATHES & E.O. LEW. 2005. *Forensic Pathology: Principles and Practice*. Academic Press.
- GAULD, S.C. 1996. Allometric patterns of cranial bone thickness in fossil hominids. *American Journal of Physical Anthropology* 100: 411–426.
- GETZ, B. 1960. Skull thickness in the frontal and parietal regions. *Acta Morphologica Neerlonda-Scandinavica* 3: 221-228.
- HATIPOGLU, H.G., H.N. OZCAN, U.S. HATIPOGLU & E.Y. YUKSEL. 2008. Age, sex and body mass index in relation to calvarial diploe thickness and craniometric data on MRI. *Forensic Science International* 182, 46-51.
- HIJMA, M.P., K.M. COHEN, W. ROEBROEKS, W.E. WESTERHOFF & F.S. BUSSCHERS. 2012. Pleistocene Rhine-Thames landscapes: geological background for hominin occupation of the southern North Sea region. *Journal of Quaternary Science* 27(1): 17-39.
- JUNG, Y.S., H.J. KIM, S.W. CHOI, J.W. KANG, & I.H. CHA. 2003. Regional thickness of parietal bone in Korean adults. *International Journal of Oral and Maxillofacial Surgery* 32(6): 638–641.
- KEEN, J.A. 1950. A study of the differences between male and female skulls. *American Journal of Physical Anthropology* 8, 65-80.
- KENNEDY, G.E. 1991. On the autapomorphic traits of Homo erectus. *Journal of Human Evolution* 20: 375–412.
- LAHR, M.M. & R.V.S. WRIGHT. 1996. The question of robusticity and the relationship between cranial size and shape in Homo sapiens. *Journal of Human Evolution* 31(2), 157-191.
- LI, H., J. RUAN, Z. XIE, H. WANG & W. LIU. 2007. Investigation of the critical geometric characteristics of living human skulls utilising medical image analysis techniques. *International Journal of Vehicle Safety* 2: 345–367.

- LIEBERMAN, D.E. 1996. How and why humans grow thick skulls: experimental evidence for systemic cortical robusticity. *American Journal of Physical Anthropology* 101: 217-236.
- LOTH, S. R. & M.Y. İŞCAN. 2000. Anthropology: Sex Determination. *Encyclopedia of Forensic Sciences* 252-260.
- MCILVAINE, B.K. 2013. Implications of reappraising the iron-deficiency anemia hypothesis. *International Journal of Osteoarchaeology* DOI: 10.1002/oa.2383.
- MEINDL, R.S. & C.O. LOVEJOY. 1985 Ectocranial suture closure: a revised method for the determination of skeletal age at death based on the lateral-anterior sutures. *American Journal of Physical Anthropology* 68(1): 57-66.
- ORTNER, D.J. 2003. *Identification of pathological conditions in human skeletal remains*. San Diego: Elsevier.
- PENSLER, J. & J.G. MCCARTHY. 1985. The calvarial donor site: an anatomic study in cadavers. *Plastic and reconstructive Surgery* 75(5), 648-685.
- REINHARD, R. & F.W. RÖSING. 1985. *Ein Literaturüberblick über Definitionen diskreter Merkmale/anatomischer Varianten am Schäde des Menschen*. Ulm: Selbstverlag.
- ROCHE, A.F. 1953. Increase in cranial thickness during growth. *Human Biology* 25-2: 81-92.
- ROSS, A.H., R.L. JANTZ & W.F. MCCORMICK. 1998. Cranial thickness in American females and males. *Journal of Forensic Sciences* 43: 267-72.
- SCHEUER, L. & S. BLACK. 2000. *Developmental Human Osteology*. Academic Press: New York.
- SCHULTZ, M., C.S. LARSEN & K. KREUTZ. 2001. Disease in Spanish Florida. Microscopy of porotic hyperostosis and inferences about health, in C.S. Larsen (ed.) *Bioarchaeology of La Florida: human biology in northern frontier New Spain*: 207-225. Gainesville: University Press of Florida.
- SPOOR, F., C. STRINGER & F. ZONNEVELD. 1998. Rare temporal bone pathology of the Singa calvaria from Sudan. *American Journal of Physical Anthropology* 107:41-50.
- STUART-MACADAM, P.L. 1987. A radiographic study of porotic hyperostosis. *American Journal of Physical Anthropology* 74: 511-520.
- 1992. Porotic hyperostosis: a new perspective. *American Journal of Physical Anthropology* 87: 39-47.
- TODD, T.W. 1924. Thickness of the male white cranium. *Anatomical Record* 27: 245-256.
- TWIESSELMANN, F. 1941. Méthode pour l'évaluation de l'épaisseur des parois cranienne. *Bulletin de la Musée Royal d'Histoire Naturelle de Belgique* 17: 1-33.

- VERCELLOTTI, G., D. CARAMELLA, V. FORMICOLA, G. FORNACIARI & C.S. LARSEN. 2010. Porotic hyperostosis in a Late Upper Palaeolithic skeleton (Villabruna 1, Italy). *International Journal of Osteoarchaeology* 20: 358–36.
- VERHAEGENA, M., & S. MUNRO. 2011. Pachyosteosclerosis suggests archaic Homo frequently collected sessile littoral foods. *HOMO - Journal of Comparative Human Biology* 62: 237-247.
- WALKER, P.L., R.R. BATHURST, R. RICHMAN, T. GJERDRUM & V.A. ANDRUSHKO. 2009. The causes of porotic hyperostosis and cribra orbitalia: a reappraisal of the iron-deficiency-anemia hypothesis. *American Journal of Physical Anthropology* 139(2): 109-125.
- WALRATH D.E., P. TURNER & J. BRUZEK. 2004. Reliability Test of the Visual Assessment of Cranial Traits for Sex Determination. *American Journal of Physical Anthropology* 125: 132-137.
- WASHBURN, S.L. 1947. The relation of the temporal muscle to the form of the skull. *The Anatomical Record* 99(3): 239-248.
- WILKINSON, C. 2004. *Forensic Facial Reconstruction*. University Press: Cambridge.
- YOUNG, R.W. 1957. Postnatal growth of the frontal and parietal bones in white males. *American Journal of Physical Anthropology* 15: 367-386.

**Figure S1. The full CT scan of the parietal, with a cross-section, and the rotating images (created by A.E. van der Merwe and J. Hagoort; see separate Figure S1).**

**Table 1: Chord and Arc Measurements (mm) of the Left Parietal Bone.**

<b>Landmarks and Locations</b>	<b>CHORD (mm)</b>	<b>ARC (mm)</b>
Lambda to anterior-superior edge of bone along sagittal suture	77.5	88.0
Lambda to Asterion	87.0	107.0
Asterion to anterior-inferior edge of bone along squamosal suture	81.8	95.0
Mid-sagittal <sup>1</sup> to mid-squamosal <sup>1</sup>	108.6	133.0
Anterior-superior edge to anterior-inferior edge	101.2	118.0

<sup>1</sup>to middle of the amount of suture that is present

**Table 2: Thickness Measurements (mm) of the Left Parietal Bone.**

<b>Location</b>	<b>Overall Thickness</b>	<b>Thickness of diploë</b>	<b>Thickness of outer plate</b>	<b>Thickness of inner plate</b>
Lambda	6.0	2.1	2.7	1.2
Posterior mid-sagittal	4.1	1.0	1.8	1.3
Mid-sagittal	5.0	1.8	2.1	1.1
Anterior mid-sagittal	6.1	3.0	1.9	1.2
Anterior-superior edge	4.8	1.6	1.7	1.5
Anterior-inferior edge	3.1	1.5	0.6	1.0
Mid-squamosal	1.0	--	--	--
Asterion	7.0	3.8	1.7	1.5
Mid-lambdoidal	7.1	2.0	3.6	1.5
Middle of the parietal eminence	6.2	3.4	2.0	0.8

## **S2. The Decorated Bovid Metatarsal**

### **Introduction**

The bone was retrieved during fishing activities in January 2005. Exact date and vessel are not known. The find location is southwest of the Brown Bank. It was collected by one of the authors (Jan Glimmerveen). The piece was sampled for radiocarbon dating and then preserved by desalination and impregnation with a solution of glue and acetone.

### **Local Geology**

The find was retrieved from the Brown Bank area of the North Sea, situated on the margin of the depocenter of the Southern North Sea Basin. The complex sedimentary sequence consists of marine, brackish-marine, deltaic and fluvial sediments. Locally, evidence of ice-pushed sediments of Elsterian and Saalian age has been documented. Lagunal and glaciolacustrine clays of the Brown Bank Member (Eem Formation) are widespread. The Pleistocene sedimentary units are overlain by Holocene marine deposits and the Basal Peat Bed. Four fauna associations from the Early Pleistocene to the Holocene have been identified in the area (Van Kolfschoten & Laban 1995).

## Methods

A sample was cut from the interior near the proximal end before the preservation of the bone. Both radiocarbon dating and stable isotope analysis were performed. The C and N content of the collagen were both in the acceptable range. The bone was measured following Von den Driesch (1976) with an analog caliper. The decoration was studied macroscopically and using a Nikon SMZ645 binocular microscope (magnification: 8-80x). One line of decoration was photographed using a Leica M80 stereozoom microscope (lens: plan 1.0x) and then studied. Further details were studied using a Hirox KH8700 microscope at the National Heritage Agency, Amsterdam. We chose not to use SEM because of the preservation of the piece and the fragile bone surface.

## Description

The bone is a large, anterior proximal part of the right metatarsus of a bovid. Approximately 50% of the length and less than half of the circumference has been preserved. The object is 164mm long, 69mm wide, 30mm thick, and weighs 213 grams (see Table 1 for measurements). Identification to the genus level is problematic, but the presence of a medial tubercle on the facet of the 2nd-3rd tarsal suggests *Bison* sp. (Gee 1993, 85-86).

The brownish-black and somewhat glossy bone surface, intensified by the impregnation with a solution of glue and acetone, is relatively well-preserved with several long cracks parallel to the length of the bone, and flaking along the cracks and on the ridges of the proximal part (weathering stage 2, following Behrensmeyer 1978, also Fernández-Jalvo & Andrews 2016). We interpret this as subaerial weathering that took place before the inundation of the North Sea. The longitudinal break is straight, smooth and brown in colour. The medial break is transverse to curved, smooth and partially black. Both breaks occurred after the decoration of the bone but at different times. The longitudinal break is clearly (sub)recent since it breaks through the black discoloration, but the medial break is much older; it is not clear whether this break occurred during handling of the bone or sometime after it was decorated. The brownish-black discoloration possibly consists of manganese dioxide (Fernández-Jalvo & Andrews 2016) or a compound of iron and sulphur (cf. black patina on flint, e.g. Stoel 1991). Bryozoa are present on the proximal end and on the medial break, both on the outside and inside. There is no evidence of carnivore tooth marks or percussion marks. There is no difference in the weathering of the decoration and the undecorated bone surface. Therefore we assume that the decoration is not much younger than the bone itself.

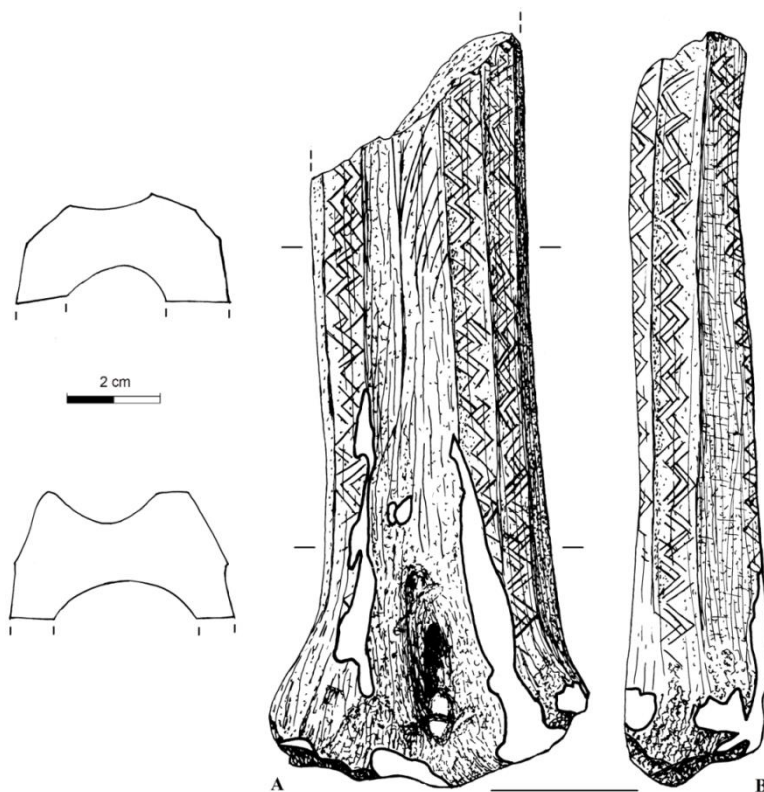
The decoration of the bone consists of five longitudinal rows of zigzags positioned on flat facets using the morphology of the bone. The decoration is best preserved on the diaphysis and appears more weathered towards the proximal end. The central anterior surface of the metatarsus is not decorated, but the surface is covered with elongated straight to curved marks, consisting of coarse and fine scratches, along the length of the bone similar to long scraping marks (cf. Fernández-Jalvo & Andrews 2016). Similar traces are present on the lateral facets and partially on the other facets. It indicates that the bone surface was prepared by scraping with a flint tool to create discrete flat facets for decoration. Since some of the marks mentioned above consist of parallel sets of scratches we have the impression that part of the scraping was done with a flint or stone tool with a retouched edge, resulting in multiple points of contact with the bone surface.

The pattern of decoration consists of five rows preserving 20/21, 14, 13, 12 and 7 complete or partial zigzags. The zigzags consist mostly of sequences of three parallel straight strokes. One row was photographed with the Leica M80 stereozoom microscope to analyse the intersection of strokes based on the depth of the cuts. The crossing of the marks, where readable, indicates that the zigzags of the row were executed from the medial to the proximal end of the bone. Detailed analysis of one row indicates a change in the strokes. The first few zigzags are very regular and formed by straight, parallel strokes with similar microtraces. The lines are closely connected forming regular and closed zigzags. After the ninth series of three strokes, the cuts become more variable. The series in the “downward” direction are more straight, parallel and regular, but the “upward” series are more variable and more curved. The zigzags become less regular and lines frequently do not overlap or connect. However, similar microtraces within individual strokes appear throughout the row suggesting that the change is not due to a change of tool, but more likely a change of gesture combined with positioning of the bone. Despite irregularities in the incisions, great care is taken to stay within the limits of the facet. The individual incisions are difficult to read because of the film of glue that prevents the bone from fragmenting. As far as current reading allows, the length of incisions varies generally between 4 and 8mm with a width of 0.2 and 0.6mm. The tracing in each stroke is probably the result of multiple incisions or the result of working with an angular tool, possibly a burin. Cross-sections vary from V-shaped to square, most likely made with a flint or stone implement. The other two more or less complete rows have been scanned for the pattern of line crossings indicating a similar execution from medial to proximal end. If the other, missing side, of the bone was decorated in a similar fashion, possibly eight decorated zones were present.

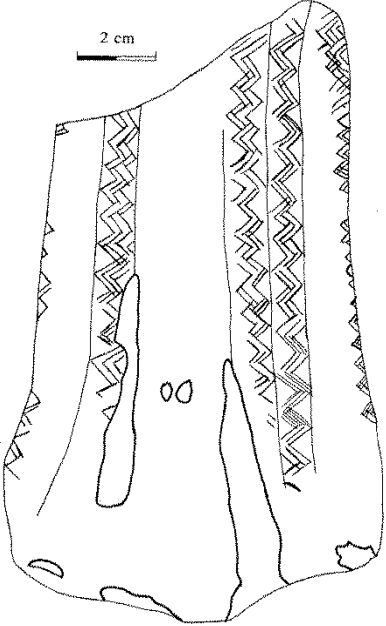
## References

- BEHRENSMEYER, A.K. 1978. Taphonomic and ecologic information from bone weathering. *Paleobiology* 4(2): 150-162.
- FERNÁNDEZ-JALVO, Y. & P. ANDREWS. 2016. *Atlas of Taphonomic Identifications*. Dordrecht: Springer.
- GEE, H. 1993. The distinction between postcranial bones of *Bos primigenius* Bojanus, 1827 and *Bison priscus* Bojanus, 1827 from the British Pleistocene and the taxonomic status of *Bos* and *Bison*. *Journal of Quaternary Science* 8-1: 79-92.
- STOEL, P. 1991. Patina-onderzoek bij vuursteen. *Archeologie* 3: 50–53.
- VAN KOLFSCHOTEN, T. & C. LABAN. 1995 Pleistocene terrestrial mammal faunas from the North Sea. *Mededelingen Rijks Geologische Dienst* 52: 135-151.
- VON DEN DRIESCH, A. 1976. *A guide to the measurement of animal bones from archaeological sites*. Cambridge (Mass.): Peabody Museum Press.

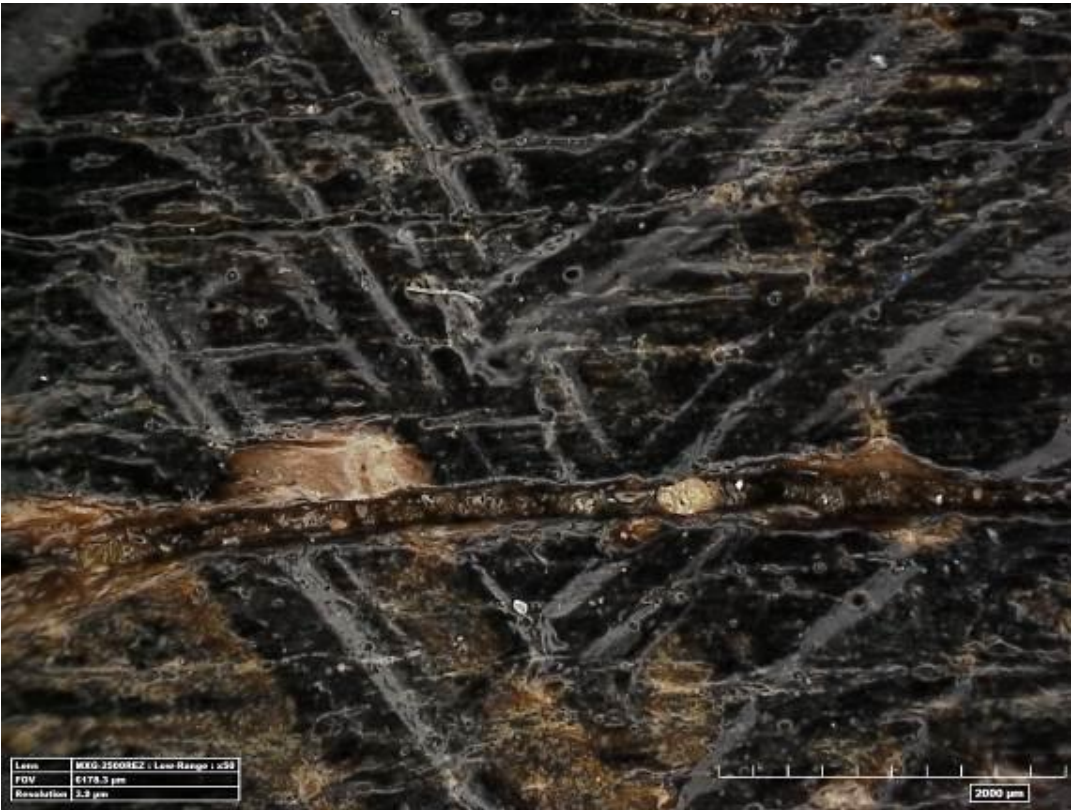
### S2 Figure 1A. Drawing of the decorated bone (L. Johansen).



S2 Figure 1B. Design of decoration, unfolded view (L. Johansen).

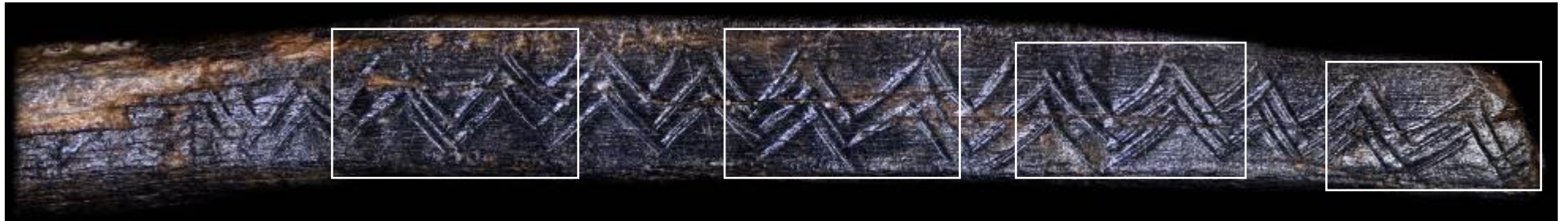


S2 Figure 2. Photographs of details, made with Hirox KH8700 microscope.

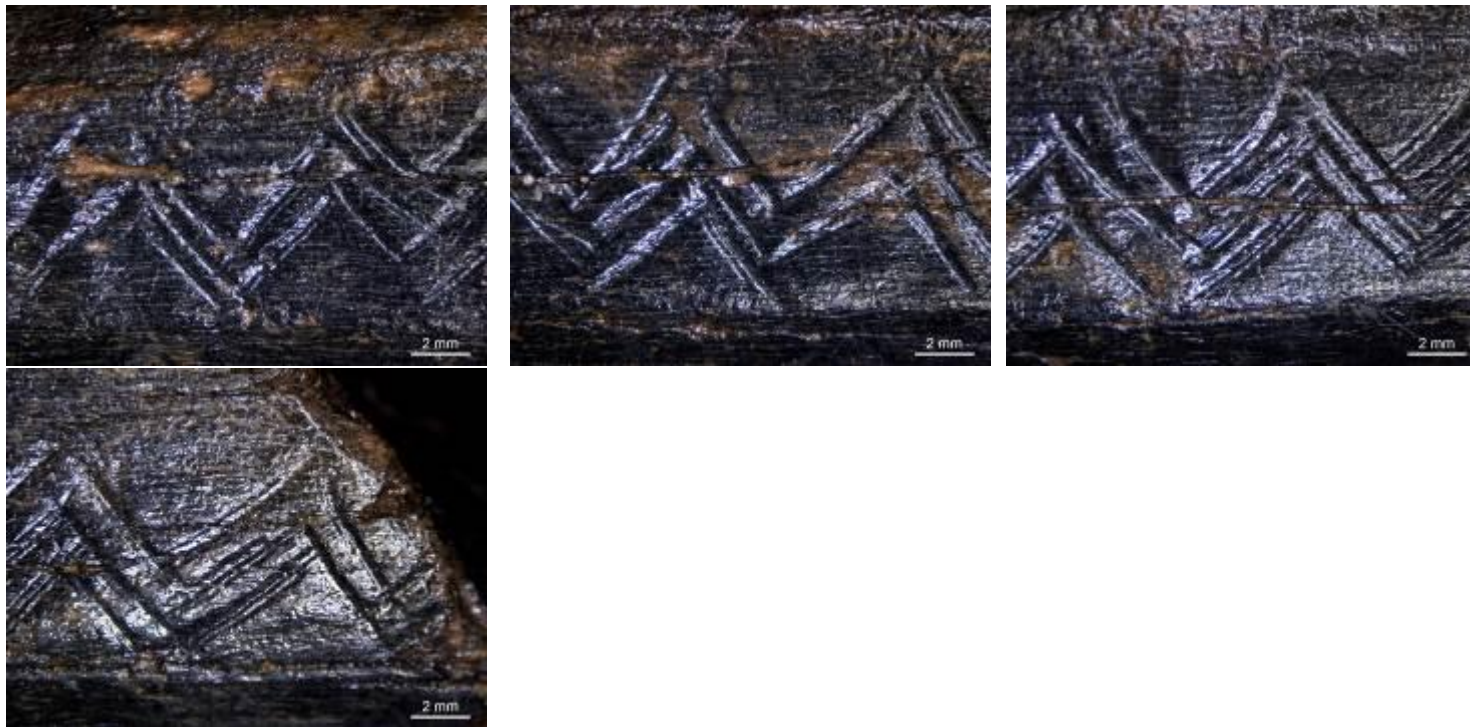


**S2 Figure 3. Photographs of details, made with Leica M80 stereozoom microscope.**

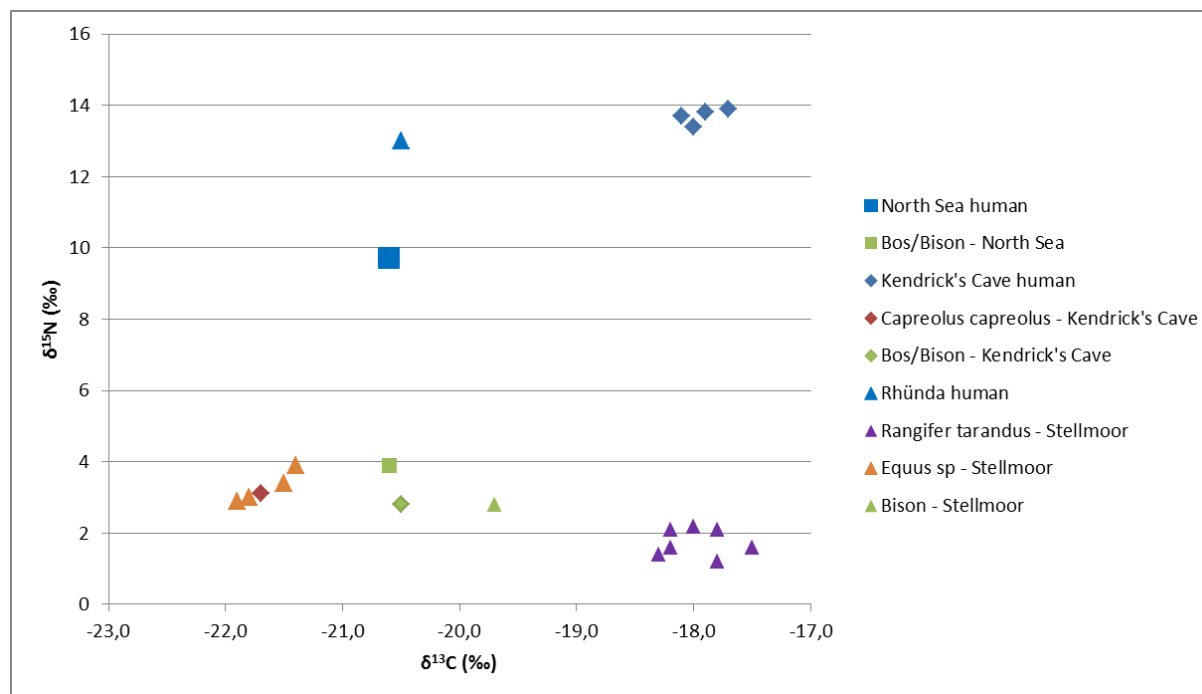
A. Panorama of one facet (created by E. Pop).



B. Details.



**S2 Figure 4. Stable isotope data and chart.**



Site	Country	Species	14C age	$\delta^{13}\text{C}$ (‰)	$\delta^{15}\text{N}$ (‰)	Reference
North Sea	Netherlands	Homo sapiens	11050 ± 50	-20,6	9,7	This paper
North Sea	Netherlands	Bos/Bison - North Sea	11560 ± 50	-20,6	3,9	This paper
Kendrick's Cave	United Kingdom	Homo sapiens	11880 ± 90	-17,9	13,8	Richards et al. 2005
Kendrick's Cave	United Kingdom	Homo sapiens	11930 ± 90	-18,0	13,4	Richards et al. 2005
Kendrick's Cave	United Kingdom	Homo sapiens	12090 ± 90	-17,7	13,9	Richards et al. 2005
Kendrick's Cave	United Kingdom	Homo sapiens	11760 ± 90	-18,1	13,7	Richards et al. 2005
Kendrick's Cave	United Kingdom	Capreolus capreolus	11795 ± 65	-21,7	3,1	Richards et al. 2005

Kendrick's Cave	United Kingdom	Bos/Bison	12410 ± 100	-20,5	2,8	Richards et al. 2005
Rhünda	Germany	Homo sapiens	10200 ± 60	-20,5	13	Drucker et al. 2015
Stellmoor	Germany	Rangifer tarandus		-18,0	2,2	Drucker et al. 2015
Stellmoor	Germany	Rangifer tarandus		-18,3	1,4	Drucker et al. 2015
Stellmoor	Germany	Rangifer tarandus		-18,2	2,1	Drucker et al. 2015
Stellmoor	Germany	Rangifer tarandus		-17,5	1,6	Drucker et al. 2015
Stellmoor	Germany	Rangifer tarandus		-17,8	1,2	Drucker et al. 2015
Stellmoor	Germany	Rangifer tarandus		-18,2	1,6	Drucker et al. 2015
Stellmoor	Germany	Rangifer tarandus		-17,8	2,1	Drucker et al. 2015
Stellmoor	Germany	Equus sp		-21,9	2,9	Drucker et al. 2015
Stellmoor	Germany	Equus sp		-21,8	3	Drucker et al. 2015
Stellmoor	Germany	Equus sp		-21,4	3,9	Drucker et al. 2015
Stellmoor	Germany	Equus sp		-21,5	3,4	Drucker et al. 2015
Stellmoor	Germany	Bison		-19,7	2,8	Drucker et al. 2015

**Table 1. Measurements for the decorated metatarsus, following Von den Driesch (1976)**

GL	Greatest length	More than 164 mm
Bp	Greatest proximal breadth	~69 mm
Dp	Greatest proximal depth	More than 30 mm
SD	Smallest diaphysal breadth	~45 mm
DD	Smallest diaphysal depth	More than 24 mm

### **S3. Information on provenance**

The objects are so-called ‘by-catches’ of beam trawling, a fishing technique no longer allowed due to European regulations. The technique uses nets weighted with metal bars, which were dragged across the sea floor to fish for sole, plaice and other bottom feeding fish. As ‘by-catch’, bones and stones (or “bonken”), end up in the fishing nets. Thanks to long-lasting cooperation between several collectors and beam trawling fishermen, all by-catches were brought ashore. The by-catch was transported to Urk, where all the fossil bones were thoroughly examined, categorised and documented. The most interesting find categories became part of private and public collections and were made available for scientific research. As part of the cooperation, crew members on board the beam trawling vessels were not only willing to cede their by-catch for research purposes, but they also provided the localities where the material was collected. By-catch was kept separated by day or week and the fishermen kept records of the areas where they dragged their nets across the North Sea floor, sometimes in lines of several kilometers long. Hence, the find location can only be indicated by approximation.

The decorated bone was recognised among the by-catch of fishing activities southwest of the Brown Bank in January 2005. Jan Glimmerveen examined, categorised and documented the object. The object was donated by Klaas Post to Jan Glimmerveen and became part of his private collection. Jan Glimmerveen sampled the bone for  $^{14}\text{C}$  dating before preserving it. The inventory number is JG 93.

The parietal was recognised among the by-catch of a specific vessel “Scheveningen 18” from June 6, 2013. The human bone was recognised and categorised by Albert Hoekman (North Sea fossils), Dick Mol, and Klaas Post. They donated the bone to the National Museum of Antiquities in Leiden (The Netherlands). The bone was sampled on September 27, 2013 for  $^{14}\text{C}$  dating and stable isotope analyses by Hans van der Plicht (Center for Isotope Research, Groningen), before preservation of the bone. The inventory number is U 2013/6.1.